Multi-zone parametric inverse analysis of super high arch dams using deep learning networks based on measured displacements

Xi Liu[1,2], Fei Kang[*,1], Maria Pina Limongelli[2]

1. School of Hydraulic Engineering, Faculty of Infrastructure Engineering, Dalian University of Technology, Dalian 116024, P. R. China

2. Department of Architecture, Built Environment and Construction Engineering, Politecnico di Milano, Piazza Leonardo da Vinci 32, 20133 Milan, Italy

Abstract

Parametric inverse analysis/identification provides significant information for structural damage detection and construction in dam engineering, The main challenge of inverse analysis is to improve the computational efficiency and accuracy for complex structures, especially for super high arch dams with many zone parameters. This study developed a high-precision deep learning-based surrogate model for rapid inverse analysis of concrete arch dams. The relationship between mechanical parameters and multi-point displacement response is interpreted by convolutional neural networks (CNN)-based surrogate model. The proposed model is integrated with the Latin hypercube sampling and a meta-heuristic optimization algorithm for rapid inverse analysis strategy. The objective function is set as distance between the measured displacement and the corresponding value predicted by the surrogate model. The proposed approach is tested on a real super high concrete arch dam. Results show that the proposed approach can achieve promising accuracy and improve the computational efficiency of the inverse analysis.

Keywords: concrete arch dams; parameter identification; inverse problem; deep learning; surrogate model;

1 Introduction

Dams are important hydraulic structures that provide water supply, flood control, irrigation, navigation, and hydropower generation. Large dam failures can have devastating consequences for the environment, society, economy, and lives. As a result, research is increasingly devoted to the diagnostic analysis and overall evaluation of dams. Due to the effect of environmental, hydraulic, and

* Corresponding author. Tel.:+86-0411-84708500; Fax: +86-0411-84708501

E-mail address: liuxidlut@163.com (X. Liu); kangfei@dlut.edu.cn, kangfei2009@163.com (F. Kang); mariagiuseppina.limongelli@polimi.it (M. Limongelli);

25 geomechanically factors, significant concrete degradation may occur, resulting in a loss of strength,
26 stiffness, and other physical properties of materials [1,2]. The identification of the current values of the
27 material parameters plays an important role in the safety assessment of concrete dams. A powerful
28 technique for the identification of the mechanical parameter of dam-foundation systems is inverse
29 analysis[3].

30 The elastic/deformation modulus of concrete dams and their foundation is a crucial parameter that
31 affects the deformation and stress of the structures. Damage in concrete dams often causes the
32 reduction of these parameters [4]. The values of these are often unavailable in the design documents or
33 may differ from those, not least due to damage. Furthermore, in large dams it difficult to measure the
34 value of the elastic modulus of concrete using on-site tests due to the need for large specimens and
35 testing machines [5]. For this reason, an inverse analysis can be the preferred choice to estimate these
36 parameters.

37 Sensors deployed on concrete dams provide essential information for the assessment of dams. The
38 pendulum system, which has the advantages of high accuracy, durability and simplicity of operation, is
39 a commonly used monitoring instrument for the measurement of horizontal displacement of concrete
40 dams and foundations [6]. An effective approach to the inverse analysis of dam material parameters is
41 based precisely on pendulum data and calculated response of finite elements (FE) under hydraulic
42 loads [7]. That is, the commonly used method for inverse analysis is as follows. Firstly, the hydraulic
43 components associated with the hydrostatic load are separated from the measured response by
44 statistical regression analysis. The hydraulic components are then compared with the FE calculated
45 response. By continuously updating the FE model so that the calculated response is close to that of the
46 hydraulic component, the true parameter values can be obtained. This method has the advantage of

47 being easy to implement since the hydraulic component depends mainly on the mechanical properties
48 of the material and is less associated with burdensome thermal analysis [8]. However, finite element
49 calculations for large concrete dam-foundation systems with many elements and degrees of freedom
50 can be time-consuming.

51 To improve the efficiency of inverse analysis, surrogate models, also known as meta-models are
52 widely implemented. The fundamental concept of surrogate modeling is to replace a computationally
53 expensive finite element analysis model with a sufficiently accurate and efficient data-driven model [9].
54 Commonly used approaches to surrogate modeling include the kriging model [10], response surface
55 methodology [11,12], and neural network-based models such as radial basis function (RBF), back
56 propagation (BP), and artificial neural networks (ANNs). Owing to the powerful ability to capture the
57 nonlinear characteristics of material parameters and structural response, the neural network-based
58 surrogate models have been successfully applied to parametric inverse analysis in dam engineering
59 [4,7,13,14]. However, traditional neural network-based surrogate models have some drawbacks. For
60 instance, they require a large set of training data in order to achieve satisfactory accuracy, but they
61 frequently suffer from overfitting problems. Different network structures must be designed and the
62 model must be retrained for different problems. Moreover, the shallow architecture of neural networks
63 restricts their ability to model complex nonlinear systems with high-dimensional data.

64 In recent years, deep learning techniques have developed. Deep learning networks (DNNs) can
65 extract and classify high-dimensional features from the input data. Moreover, the cost of retraining the
66 model using similar data is lower with respect to shallow neural networks since new models can be
67 developed by fine-tuning existing DNNs. The applicability of DNNs-based surrogate modeling has
68 been demonstrated in a variety of fields, including one-way slab design and optimization [15],

building's structural seismic response prediction [16,17], and geotechnical reliability analysis [18]. In dam engineering, DNNs have been successfully applied to displacement prediction modeling based on monitoring data [19,20].

In general, the surrogate model is combined with optimization algorithms for the parametric inverses analysis. Metaheuristic optimization algorithms such as genetic algorithm (GA)[21,22], particle swarm optimization (PSO)[23,24] and their improved forms have been widely used in inverse analysis due to their good global search ability. Recently, a novel one called Jaya[25] has been successfully applied to the optimization inverse analysis of dam-foundation systems[26,27]. Jaya algorithm has a simple structure and fast convergence, and it has shown promising performance in a variety of engineering optimization problems. In this paper, Jaya algorithm is utilized for inverse analysis of multi-parameter, and its performance is investigated.

The deformation behavior of concrete high arch dams under normal conditions has a strong spatial correlation [28]. On the other hand, material parameters vary across the structure due to the uncertainty of the construction process. In literature the inverse problem for large structures is gradually becoming focused on the identification of parameters relevant to spatial partition of the structure in an effective and timely manner. Labibzadeh[29] proposed a thermal inverse analysis method for determining the elastic properties of an old concrete arch dam considering the effect of interaction between vertical adjacent blocks of an arch dam. Bao[30] performed inverse analysis of multiple mechanical parameters of a high arch dam based on multioutput least-squares support vector regression machine and improved differential evolution algorithm. Wang[31] proposed a hydraulic, exponential, seasonal and temporal (HEST) statistical model-based multi-point zonal viscoelastic parameter inversion method for high arch dams.

The purpose of this paper is to achieve rapid and efficient inverse analysis of a high arch dam-foundation system with multiple spatial parameters. To this end, the use of DNNs-based surrogate model instead of FE model is investigated. The architecture of DNN adopted for surrogate modeling is based on convolutional neural networks (CNN). CNN is one of the most successful deep learning algorithms used for image processing in the computer science community[32]. Aside from that, CNN has been successfully applied in civil engineering to response evaluation[33] and damage detection[34,35] in large-scale structures. The basic idea behind the research presented in this paper is to (1) exploit the CNN capabilities for spatial feature extraction to construct a CNN-based deep learning surrogate model for mapping the relationship between the multi-spatial zone parameters and the structural response of the dam in terms of displacement, (2) to define the objective function of the inverse analysis in terms of dam displacements monitored at multiple locations and the displacements provided by the CNN model, (3) to minimize the objective function using Jaya optimization algorithm.

The remainder of this paper is structured as follows. Section 2 provides the general paradigm for the inverse analysis of concrete arch dams. Section 3 introduces the theory and the procedure of the proposed approach. Section 4 presents the application to a case study, and Section 5 summarizes the finding of this study.

2 General paradigm for inverse analysis of concrete arch dams

2.1 Solution strategies for inverse problems

In general, the structural response used for the inverse analysis is computed using a FE model that computes the structural response based on the assigned values of the mechanical parameters. It is assumed that the dam and foundation are in an elastic state under the hydrostatic load, and the materials are homogeneous and isotropic. The equilibrium equation of the structural model based on FE method

can be expressed as Eq. (1)

$$\mathbf{K} \cdot \boldsymbol{u} = \boldsymbol{R} \tag{1}$$

where **K** is the overall stiffness matrix, $\boldsymbol{u}$ is the nodal displacement vector, and $\boldsymbol{R}$ is the load vector.

The overall stiffness matrix **K** is determined by the material properties and it can be formulated as Eq. (2)

$$\mathbf{K} = \iiint_{\Omega} \mathbf{B}^{\mathrm{T}} \mathbf{D} \mathbf{B} \, \mathrm{d}\Omega \tag{2}$$

where **B** is the strain–displacement matrix, Ω is the calculation domain of FE method, $\mathbf{D}=f(E, \mu)$ is the stress–stain matrix, E is the elastic/deformation modulus, μ is the Poisson's ratio. The latter plays a minor role in the overall response of the dam thereby herein is assumed to be known a priori and constant.

The displacement under the hydrostatic load depends on the reservoir level fluctuations and on the values of the elastic/ deformation modulus. To define the objective function in terms of the difference between the monitored displacements and the displacements calculated by the FE model, the latter must be calculated considering the same water reservoir level. The elastic/ deformation modulus are identified minimizing the objective function defined as Eq. (3)

$$J(\boldsymbol{E}) = \omega_i \sum_{i=1}^{N_P} \left(\left(u_{h,i}^{*}(\boldsymbol{E}) - u_{h,i} \right) / u_{h,i} \right)^2 \tag{3}$$

where $\boldsymbol{E}$ is the vector of elastic/ deformation modulus to be determined, ω_i is the weight, N_P is the number of monitoring points, $u_{h,i}$ is the hydrostatic component of ith monitoring point, $u_{h,i}^{*}$ is the structural response calculated by the FE method.

The inverse problem of the dam-foundation system can be defined as:

$$\begin{cases} \min \;\; J(\boldsymbol{E}) = \omega_i \sum_{i=1}^{N_P} \left(\left(u_{h,i}^{*}(\boldsymbol{E}) - u_{h,i} \right) / u_{h,i} \right)^2 \\ \text{s.t.} \;\; \mathbf{K} \cdot \boldsymbol{u} = \boldsymbol{R} \\ E_{j,\min} \le E_j \le E_{j,\max} \;\; \left(j = 1,\ 2,\ \cdots,\ N_E \right) \end{cases} \tag{4}$$

where s.t. stands for subject to, N_E is the number of parameters to identify, $E_{j,\,\min}$ and $E_{j,\,\max}$ is the minimum and maximum boundary values of the jth parameter, respectively. The values for these two are determined based on the design specifications and relevant literature.

2.2 Mathematical model for measured displacement analysis

The displacement response depends on the effect of external loads and on the value of the mechanical parameters previously defined. Also as described earlier, the commonly used inverse analysis method is based on hydraulic component data and computed response data from FE model. In this case, the hydraulic components are separated from the measured displacement by statistical regression analysis.

In this paper, the hydrostatic-seasonal-time (HST) statistical model is adopted for dam displacement analysis. The HST model is widely used in practice for interpreting dam displacement responses[36]. The measured dam displacement u in the HST model is assumed to be composed of three components, which are (1) the reversible hydrostatic component u_h due to the changes in reservoir level, (2) the seasonal thermal component u_s caused by seasonal change in ambient temperature, (3) the irreversible time component u_θ associated with concrete creep and alkali-aggregate reaction. The HST model can be expressed in Eq. (5)

$$u = u_h + u_s + u_\theta \tag{5}$$

The hydrostatic component in Eq. (5) for concrete arch dams is formulated as[36]

$$u_h = a_1 h + a_2 h^2 + a_3 h^3 + a_4 h^4 \tag{6}$$

where h is the reservoir level, a_1, a_2, a_3, and a_4 are the model coefficients.

The commonly used formula of thermal component is based on the harmonic functions[37] as given in Eq. (7)

$$u_s = b_1 \sin(s) + b_2 \cos(s) + b_3 \sin^2(s) + b_4 \sin(s)\cos(s) \tag{7}$$

where s is a variable that varies seasonally in relation to the annual frequency, s= 2πk/365.25, k is the number of days from the beginning of monitoring date to the observation date, and b_1 to b_4 are the model coefficients.

The irreversible time component can be expressed as a combination of time-dependent monotonic functions[38]. Many different functions have been proposed in literature such as the sum of linear and exponential terms[36,37,39], linear and logarithmic terms[40,41], or only linear form[42]. The exponential function, as shown in Eq. (8) is recommended due to the significant irreversible deformation associated with time during the initial service life of the concrete arch dam.

$$u_\theta = c_0\left(1 - e^{-c_1\theta}\right) \tag{8}$$

where θ is the number of days from initial operation to observation date, c_0, c_1 are the model coefficients. It should be mentioned that the value of c_1 in Eq. (8) is not uniform and is commonly determined empirically. To determine the value of c_1, a simple and effective method known as the random search algorithm[43] (RSA) is applied in this study.

3 Methodology

3.1 Proposed framework and procedure

The proposed framework for multi-zone parametric inverse analysis is mainly divided into four phases: data analysis and preparation, CNN-based surrogate model for displacement prediction, optimization/inverse analysis, and performance evaluation of the proposed approach. Fig. 1 illustrates

the flowchart of the proposed framework, which consists primarily of seven steps summarized as follows.

Step 1: Analyze the monitoring data. The hydrostatic component (as a term of the objective function) is separated from the measured displacement based on the multiple linear regression (MLR) techniques.

Step 2: Create a FE model with high precision. An appropriate FE model is developed to accurately simulate the relationship between mechanical parameters and structural response.

Step 3: Establish the dataset. The Latin hypercube sampling (LHS) [44] method is used to generate parameter sample data, which is then fed into the FE model to obtain the corresponding displacement data. In this way, the dataset of parameters and displacement data is established.

Step 4: Develop the CNN-based surrogate model. The architecture of the CNN is constructed. The surrogate model is developed using the dataset and the best-fitting model is selected to replace the FE model for displacement prediction.

Step 5: Inverse analysis for the identification of the mechanical parameters. The CNN-based surrogate model is integrated with the Jaya optimization algorithm to minimize the objective function and identify the parameters based on the monitored dam response.

Step 6: Output the inverse analysis results. When the number of iterations reaches the maximum number set, the process is terminated and the parameters are output.

Step 7: Performance evaluation. The reliability of the proposed approach is verified by updating the FE model with the identified parameters and comparing the FE calculated displacements with the measured ones. If the error in terms of relative displacement is lower than 3%, the results of the inverse analysis results are deemed acceptable.

3.2 Dataset establishment

In this paper, the dataset was established based on the FE model and sampling techniques. The dataset was then separated into two subsets for training and testing the surrogate prediction model. In the surrogate model, the values of the elastic/deformation modulus are the input variables and the dam displacement is the output variable. The input variables are generated by applying the LHS method. LHS is widely used in the generation of controlled random samples since it allows the extraction of samples distributed uniformly across the sample space. Previous studies have shown that LHS can significantly save computer effort compared to classical random sampling methods[45]. Therefore, the LHS is employed to generate the initial points for the input variables within the parametric domain. After obtaining the input variables, an FE model was built to compute the displacements and use them as output data of the CNN-based surrogate model. The established FE model should have high simulation accuracy, allowing it to relate dam structural response to mechanical properties under a given load.

3.3 CNN-based surrogate model

CNN belongs to the class of ANNs, which are widely applied in various fields such as visual image analysis, natural language processing, and time series analysis. One of the most significant advantages of CNN over traditional neural networks and other DNNs is its powerful ability to automatically extract and learn features from the data using convolutional kernels. There are three types of CNN according to the dimensions of the convolutional kernel, namely one-dimensional (1D), two-dimensional (2D), and three-dimensional (3D) CNNs. The most widely used is 2D CNN, which has achieved great success in image classification problems. In recent years, 1D CNN has been developed and proven to be effective in dealing with sequence data and signal data [46]. Moreover, the 1D CNN model has

lower computational complexity and cost than 2D CNN since there is no need to transform the data into images. Previous research[20] has shown that 1D CNN can extract local trends and spatial features associated with the monitored response. This research investigates the performance of 1D CNN as a surrogate prediction model able to substitute the FE model in mapping the structural response to the mechanical parameters of the dam.

3.3.1 Architecture of the CNN model

The architecture of the CNN model is shown in Fig. 2. The network is made up of fundamental deep learning layers, including an input layer, three convolutional layers (Conv1, Conv2, Conv3) followed by three Rectified Linear Units (ReLU), two fully connected layers (FC1, FC2) and a regression layer. The three convolutional layers have the same size of filter with a width of 3, and the number of filters is 64, 128, and 256, respectively. The hyperparameters of the CNN were determined empirically or by default. Specifically, hyperparameters are determined by starting with some default values and then tuning them through empirical testing, in which different hyperparameter settings are used to train the model and the performance of the model is evaluated on a test set. The hyperparameters that result in the best performance on the test set are then selected for the CNN model. The details of the hyperparameters used in this paper are listed in Table 1.

3.3.2 Normalization

To achieve more stable and fast network training and to avoid the network assigning unrealistic importance and bias to certain variables, it is important to normalize the datasets used for the training and evaluation phases [47]. The normalization scheme adopted in this study rescales each variable to bring it in the range [0,1] as shown in equation (9).

$$\boldsymbol{x}_{\text{normal}} = \frac{\boldsymbol{x} - \min(\boldsymbol{x})}{\max(\boldsymbol{x}) - \min(\boldsymbol{x})} \tag{9}$$

where $\boldsymbol{x}_{\text{normal}}$ is the normalized variable vector, $\boldsymbol{x}$ is the variable vector, max($\boldsymbol{x}$) and min($\boldsymbol{x}$) are respectively the highest and the lowest value of the variable. To obtain the prediction results of the model at the original scale and compare them with the measured values, it is necessary to apply inverse normalization to the data.

3.3.3 Performance Criteria

The parameters adopted to define the performance criteria of the proposed CNN surrogate model are the mean absolute error (MAE), the root mean squared error (RMSE), and the coefficient of determination (R^2), defined in Eqs. (10) to (12), respectively.

$$\text{MAE} = \frac{1}{N}\sum_{i=1}^{N}|y_i - \hat{y}_i| \tag{10}$$

$$\text{RMSE} = \sqrt{\frac{1}{N}\sum_{i=1}^{N}(y_i - \hat{y}_i)^2} \tag{11}$$

$$R^2 = 1 - \frac{\sum_{i=1}^{N}(y_i - \hat{y}_i)^2}{\sum_{i=1}^{N}(y_i - \bar{y}_i)^2} \tag{12}$$

where y_i is the true target value, $\hat{y}_i$ is the predicted value, $\bar{y}_i$ is the mean value of the total y_i, N is the number of output targets. Threshold values of MAE and RMSE are set to define the performance criteria. The accuracy of the model is deemed sufficient when the MAE and RMSE are both below the threshold and R^2 (with varies in the range [0 1]) is close to 1.

3.4 Optimization algorithm

3.4.1 Jaya optimization algorithm

Jaya is a global population search-based meta-heuristic intelligent optimization algorithm. Previous studies in the literature [26,27] have demonstrated the good performance of Jaya in inverse analysis of material and dynamic parameters for concrete dams. Therefore, Jaya is applied in this study to minimize the objective function.

At k-th step of the procedure (k=1, 2, …, N_K where N_K is the maximum number of iterations, the candidate solution $p_{i,j}$ (i=1, 2, …, N_D, j= 1,2, …, N_S, N_D is the number of optimization variables and N_S is the number of solutions) are updated based on the fitness evaluation results. Specifically at each step the best solutions $p_{i,\text{best}}$ and worst solutions $p_{i,\text{worst}}$ that correspond to the optimal and worst fitness values are recorded, and the new solution $p_{i,j}^{\text{new}}$ is trended towards the optimal and away from the worst by Eq. (12).

$$p_{i,j}^{\text{new}} = p_{i,j} + r_{1,j}\left(p_{i,\text{best}} - \left|p_{i,j}\right|\right) - r_{2,j}\left(p_{i,\text{worst}} - \left|p_{i,j}\right|\right) \tag{12}$$

where $r_{1,j}$ and $r_{2,j}$ is uniformly distributed random values between [0 1].

The pseudocode of Jaya algorithm is shown in Fig. 3.

3.4.2 Optimization objective function

As mentioned in Section 2, parametric inverse analysis of dams based on measured displacements is a typical optimization process. In this paper, optimization is performed to solve the inverse problem after a high-precision surrogate model has been established. The optimization involves the minimization of the difference between the measured displacement and the displacement predicted by the surrogate model. In this paper, the objective function is defined as the absolute relative

displacement error that is the absolute value of the difference between calculated and measured displacements, normalized to the measured value. It is noted that the hydrostatic component of displacement can only be defined in a relative sense with respect to a reference reservoir level. For this reason, Eq. (13) features $\Delta u_{h,i}$ which is the difference between the values of the hydrostatic (h) components measured at location *i*, at two reservoir levels. Thus, the objective function in Eq. (4) can be redefined as

$$O(\boldsymbol{E}) = \min \sum_{i=1}^{N_P} \left| \left(\Delta u_{h,i}^{*}(\boldsymbol{E}) - \Delta u_{h,i} \right) \Big/ \Delta u_{h,i} \right| \tag{13}$$

where O (.) is the objective function, $\boldsymbol{E}$ is the vector of variables to identify (e.g. the elastic/deformation moduli), $\Delta u_{h,i}^{*}$ is the relative displacement predicted by the surrogate model, $\Delta u_{h,i}$ is the relative displacement measured at the same location, N_P is the number of monitored locations (e.g. the locations where displacements are measured).

4 Case analyses

This section presents the results obtained applying the proposed framework for parametric inverse analysis to super high concrete arch dam. To demonstrate the performance of the proposed CNN-based surrogate model, a comparison was performed by applying the CNN and the traditional shallow neural network including BP, and RBF to the same datasets. The training parameters of the BP and RBF model are determined using the RSA to obtain the optimal model performance. The performance of the Jaya optimization algorithm combined with CNN-based surrogate model is also compared to the performance of other optimization algorithms such as PSO and GA. All optimization algorithms were run 30 times independently with 300 iterations each. The initial conditions are changed by random initialization in each independent run. The computation of the structural displacement response based on FE analysis was carried out using ANSYS18.1. The CNN model and all algorithms are programmed

using MATLAB 2020b on a workstation with a 64-bit operating system, 16 GB of RAM, and an Intel(R) Core (TM) i7 CPU.

4.1 Description of case study and monitoring data

The Xiluodu hydroelectric power station is located on the mainstream of Jinsha River in southwest China. The hydropower station has been in operation since July 2013. With a total installed capacity of 13.86 gigawatts, it is the third largest hydropower station in the world. The dam is a concrete double-curved arch structure that was constructed in April 2007 and was completed in March 2014. The maximum height of the dam is 285.5m making it the third-highest arch dam in China. The bottom elevation is 324.5m, the crest elevation is 610m, and the arc length of the center line is 681.51m. It is composed of 31 concrete blocks separated by vertical and horizontal contraction joints. Fig. 4 depicts an aerial view of the dam. The reservoir was first impounded on May 4, 2013, and its normal reservoir level is 600 meters above sea level. The change in upstream reservoir water level over time is illustrated in Fig. 5. For the purposes of the study reported in this paper the dam body is partitioned into three zones (A, B, and C) built with concrete with design strengths of C40, C35, and C30. The main zones of dam are shown in Fig 6.

A pendulum system is installed on the dam to provide real-time monitoring of horizontal displacements (in both the radial and the tangential directions) and capture their evolution over time. As shown in Fig. 7, the pendulum system consists of seven groups of direct (PL) and inverted (IP) pendulums for a total of 37 monitored points located in the dam blocks 5, 10, 15, 22, and 27, on the left and on the right dam banks, respectively.

To verify the performance of the proposed approach, the horizontal radial displacement of the monitored locations (located at different elevation galleries) PL10-2, PL10-3, PL10-5, PL15-1, PL15-2,

PL15-4, PL15-5, PL22-1, PL22-2, PL22-4 are considered. The time histories of the horizontal radial displacements at these locations are presented in Fig. 8.

In this study, displacements measured from 2014 to 2018 including 721 data groups were used for displacement analysis modeling. The 550 groups of data recorded from July 6, 2014 to January 24, 2018 were used for model training, and the remaining 171 groups were used to test the performance of the model.

4.2 Displacement component separation

The HST statistical models coupled with the MLR technique were applied for displacement component separation. The performance parameters defined in section 3.3.3. are listed in Table 2 for the selected locations. The results show that the HST model is highly accurate, with an RMSE of less than 2 mm for both the training and test sets. The displacement components at various locations are shown in Fig. 9 together with the measured displacements The comparison clearly shows that the hydrostatic component accounts for a large proportion of the total displacement and has a strong correlation with the measured displacement. This confirms the feasibility of the hydrostatic component as an objective function term for the inverse analysis.

4.3 Sample datasets preparation

Each sample of the training dataset contains 17 variables, 6 of which are elastic/deformation moduli and the remaining 11 are the relative hydrostatic displacement components at two different water levels. The six elastic/deformation modulus are the parameters to identify through the inverse analysis. The water level of 550.55 m on August 12, 2015 and 599.41m on October 12, 2015 were chosen for the preparation of the dataset. Based on previous research, the size of the dataset was fixed to 600 samples

for the training set and 150 samples for the test set. In the literature [26], it is recommended to set the training sample size to 60~100 times the number of parameters to identify and the test sample size to 25% of the training size for practical engineering cases. In this study, the training sample size was set as 100 times the number of parameters to identify.

The LHS method was applied to generate the set of six elastic/deformation moduli. The pairwise distribution of the sample sets for training and test are shown in Fig. 10. The elastic modulus of the dam is given by E_A, E_B, and E_C in the range of [40 60] GPa, [35 55] GPa, and [30 50] GPa, respectively. The deformation modulus of the foundation is represented by E_{r1}, E_{r2}, and E_{r3} with ranges of [20 50]. It can be seen that the sample points are evenly distributed across the range of each variable, indicating that the sample has good spatial coverage.

The relative hydrostatic components in the sample datasets were calculated by FE analysis. Fig. 11 illustrates the FE mesh and the parameter settings. The FE model contains 28164 elements and a total of 127055 nodes. The depth and thickness of the foundation were modeled to be 1.5 times the height of the dam. The model is simplified to improve computational efficiency. Local coordinates of the FE model were created at the same locations where the sensors were deployed to make the computed FE response consistent with the measured data.

4.4 Performance of the proposed approach

The sample datasets obtained as described in Section 4.3 were used for training and test the CNN-based surrogate model. The information on the model architecture and hyperparameter settings is provided in Section 3.3.1. The displacement predicted by the surrogate model was compared to the calculated value obtained by the FE model. The results of the comparison are shown in Fig. 12. It can be observed that the predicted hydrostatic components displacement obtained by the surrogate model

and the calculated values from the finite element model are nearly identical for all monitoring points. The values of RMSE and R^2 are 0.0156 and 1 for training set, 0.0244 and 1 for test set. This suggests that the proposed surrogate model can reasonably replace the FE model in interpreting the relationship between dam displacements and material parameters.

The outcome of the surrogate model in terms of relative displacements is used in the Jaya optimization algorithm to identify the unknown structural parameters. The parameter values are assumed as the average of 30 independent runs with 300 iterations each. Fig. 13 shows the evolution of the parameter values with the number of iterations. The small variation in the parameter indicates that the results are relatively stable. The final values of the parameter are E_A=53.799GPa, E_B=45.733GPa, E_C=37.374GPa, E_{r1}=39.657GPa, E_{r2}=24.816GPa, and E_{r3}=42.359GPa.

To verify the reliability of the results obtained from the proposed approach, the parameters were input into the FE model for displacement calculation. Table 3 compares the displacements calculated from the inverse analysis results to the measured values. The maximum absolute error at all the monitoring points is less than 0.5mm, and the relative error is less than 3%. It proves that the inverse analysis parameters obtained by the proposed method are reasonable.

The execution time of the proposed method was compared with the time required by the FE method to demonstrate the computational efficiency of the proposed approach. Different from the finite element method that requires time only to minimize the objective function, the proposed approach requires time also for sample preparation. The comparison of the computational time relevant to the two methods for the same number of iterations over the evaluation of the objective function is reported in Table 4, which shows that the proposed approach improves computation efficiency by 95.83%.

4.5 Comparative study of different methods

393 *4.5.1 Comparison of different surrogate models*

394 The performance of the CNN-based surrogate model was validated by comparing it to the
395 commonly used shallow neural network BP and RBF. The training parameters of the BP and RBF
396 models were optimized by the RSA. The prediction performance comparison of different models on the
397 same sample datasets is listed in Table 5. The results show that the CNN model has the highest
398 prediction accuracy on both the training and test sets. The performance was improved by more than
399 76.36% and 86.12% compared with the BP model and RBF models, respectively.

400 *4.5.2 Comparison of different optimization algorithms*

401 The performance of the Jaya algorithm was verified by comparing it with the widely used
402 optimization algorithms PSO and GA. The evaluation process of best mean fitness for the three
403 algorithms (all coupled with the CNN-based model) is illustrated in Fig. 14. Thanks to the integration
404 with CNN all three algorithms have low fitness values however the lowest is achieved with Jaya that
405 outperforms the other two algorithms.

406 *4.5.3 Comprehensive comparison of different methods*

407 A comprehensive comparison of different methods, including Jaya-CNN, PSO-CNN, GA-CNN,
408 Jaya-BP, and Jaya-RBF, was performed to further evaluate the performance of the proposed method.
409 Parameters obtained by different methods range from about 1 GPa to 4 GPa as shown in Table 6. Their
410 discrepancy is due to the fact that the five methods have different accuracy.

411 To further test the performance of each method, the parameter results were fed into a FE model to
412 perform a forward analysis and the calculated displacements were compared to the measured ones. The
413 average absolute/relative error of each method is listed in Table 7, and the relative error of each
414 monitoring point is shown in Fig. 15 showing the superior performance of the proposed method.

5 Conclusions

This paper presents a CNN-based surrogate model coupled with an optimization algorithm for multi-parameter inverse analysis of super high arch dams. A high-precision CNN-based surrogate model was developed to interpret the relationship between the mechanical parameters and structural response of concrete dams. The objective function is defined as the relative error between the responses in terms of displacement predicted by the surrogate model and the responses measured at the monitored locations. The objective function is minimized using the Jaya optimization algorithm. The proposed method is applied to a real concrete arch dam. The following conclusions were drawn from the analysis of this case study.

- CNN is a promising tool in spatial response feature extraction for high arch dams. Even with a simple architecture, the CNN model in this study performs well for multipoint displacement prediction. The RMSE and R^2 of the CNN-based surrogate model are 0.0156 and 1 for the training set, 0.0244 and 1 for the test set. Compared with the shallow neural network BP and RBF, the CNN-based surrogate model significantly improved prediction accuracy. The prediction performance was improved by more than 76.36% and 86.12%, respectively.
- The CNN-based surrogate model replaced the FE model for muti-zone parametric inverse analysis. The proposed surrogate model combined with the Jaya optimization algorithm provides an efficient and rapid approach for parametric inverse analysis for arch dams. Compared with the direct FE method, the computational efficiency of inverse analysis improved by 95.83%.
- The parameters values obtained by the proposed approach are E_A=53.799GPa, E_B=45.733GPa, E_C=37.374GPa, E_{r1}=39.657GPa, E_{r2}=24.816GPa, and E_{r3}=42.359GPa. These parameters were input into the FE model to calculate displacement. For each monitored location, the maximum

absolute and relative errors between calculated and measured displacements are lower than 0.5 mm and 3%, respectively. The high accuracy proved that the results of inverse analysis by the proposed approach are acceptable.

- In this study, the relatively simple architecture of the CNN can also achieve high-accuracy prediction. This indicates the potentially more powerful performance of deep learning networks. In future work, the hyperparameters optimization methods for CNN networks and transfer learning-based CNN for the parametric inverse analysis in dam engineering will be investigated.

Acknowledgments

This work was supported by the National Key R & D Program of China (2022YFB4703404), the National Natural Science Foundation of China (52079022), the Fundamental Research Funds for the Central Universities (DUT21TD106), the China Scholarships Council (No. 202206060068).

References:

[1] Ardito R, Cocchetti G. Statistical approach to damage diagnosis of concrete dams by radar monitoring: Formulation and a pseudo-experimental test. Eng Struct 2006;28:2036–45. https://doi.org/10.1016/j.engstruct.2006.04.001.

[2] De Sortis A, Paoliani P. Statistical analysis and structural identification in concrete dam monitoring. Eng Struct 2007;29:110–20. https://doi.org/10.1016/j.engstruct.2006.04.022.

[3] Kang F, Li J, Xu Q. Structural inverse analysis by hybrid simplex artificial bee colony algorithms. Comput Struct 2009;87:861–70. https://doi.org/10.1016/j.compstruc.2009.03.001.

[4] Fedele R, Maier G, Miller B. Identification of elastic stiffness and local stresses in concrete dams by in situ tests and neural networks. Struct Infrastruct Eng 2005;1:165–80. https://doi.org/10.1080/15732470500030513.

[5] Vilardell J, Aguado A, Agullo L, Gettu R. Estimation of the Modulus of Elasticity for Dam Concrete. Cem Concr Res 1998;28:93–101. https://doi.org/10.1016/S0008-8846(97)00214-7.

[6] Liu X, Kang F, Ma C, Li H. Concrete arch dam behavior prediction using kernel-extreme learning machines considering thermal effect. J Civ Struct Health Monit 2021. https://doi.org/10.1007/s13349-020-00452-x.

[7] Fedele R, Maier G, Miller B. Health Assessment of Concrete Dams by Overall Inverse Analyses and Neural Networks. Int J Fract 2006;137:151–72. https://doi.org/10.1007/s10704-006-6582-7.

[8] Sevieri G, Andreini M, De Falco A, Matthies HG. Concrete gravity dams model parameters updating using static measurements. Eng Struct 2019;196:109231. https://doi.org/10.1016/j.engstruct.2019.05.072.

[9] Barhemat R, Mahjoubi S, Li VC, Bao Y. Lego-inspired reconfigurable modular blocks for automated construction of engineering structures. Autom Constr 2022;139:104323. https://doi.org/10.1016/j.autcon.2022.104323.

[10] Kleijnen JPC. Kriging metamodeling in simulation: A review. Eur J Oper Res 2009:10.

[11] Simpson TW, Poplinski JD, Koch PN, Allen JK. Metamodels for Computer-based Engineering Design: Survey and recommendations. Eng Comput 2001;17:129–50. https://doi.org/10.1007/PL00007198.

[12] Khuri AI, Mukhopadhyay S. Response surface methodology. Wiley Interdiscip Rev Comput Stat 2010;2:128–49. https://doi.org/10.1002/wics.73.

[13] Yu Y, Zhang B, Yuan H. An intelligent displacement back-analysis method for earth-rockfill dams. Comput Geotech 2007;34:423–34. https://doi.org/10.1016/j.compgeo.2007.03.002.

[14] Dou S, Li J, Kang F. Health diagnosis of concrete dams using hybrid FWA with RBF-based surrogate model. Water Sci Eng 2019;12:188–95. https://doi.org/10.1016/j.wse.2019.09.002.

[15] Ferreiro-Cabello J, Fraile-Garcia E, Martinez de Pison Ascacibar E, Martinez-de-Pison FJ. Metamodel-based design optimization of structural one-way slabs based on deep learning neural networks to reduce environmental impact. Eng Struct 2018;155:91–101. https://doi.org/10.1016/j.engstruct.2017.11.005.

[16] Zhang R, Liu Y, Sun H. Physics-guided convolutional neural network (PhyCNN) for data-driven seismic response modeling. Eng Struct 2020;215:110704. https://doi.org/10.1016/j.engstruct.2020.110704.

[17] Torky AA, Ohno S. Deep learning techniques for predicting nonlinear multi-component seismic responses of structural buildings. Comput Struct 2021;252:106570.

https://doi.org/10.1016/j.compstruc.2021.106570.
[18] Wang ZZ. Deep Learning for Geotechnical Reliability Analysis with Multiple Uncertainties. J Geotech Geoenvironmental Eng 2022;148:06022001. https://doi.org/10.1061/(ASCE)GT.1943-5606.0002771.
[19] Ren Q, Li M, Li H, Shen Y. A novel deep learning prediction model for concrete dam displacements using interpretable mixed attention mechanism. Adv Eng Inform 2021;50:101407. https://doi.org/10.1016/j.aei.2021.101407.
[20] Li Y, Bao T, Gao Z, Shu X, Zhang K, Xie L, et al. A new dam structural response estimation paradigm powered by deep learning and transfer learning techniques. Struct Health Monit 2022;21:770–87. https://doi.org/10.1177/14759217211009780.
[21] Levasseur S, Malécot Y, Boulon M, Flavigny E. Soil parameter identification using a genetic algorithm. Int J Numer Anal Methods Geomech 2008;32:189–213. https://doi.org/10.1002/nag.614.
[22] Guo Q, Pei L, Zhou Z, Chen J, Yao F. Response surface and genetic method of deformation back analysis for high core rockfill dams. Comput Geotech 2016;74:132–40. https://doi.org/10.1016/j.compgeo.2016.01.001.
[23] Chi S, Ni S, Liu Z. Back Analysis of the Permeability Coefficient of a High Core Rockfill Dam Based on a RBF Neural Network Optimized Using the PSO Algorithm. Math Probl Eng 2015;2015:1–15. https://doi.org/10.1155/2015/124042.
[24] Yang L, Su H, Wen Z. Improved PLS and PSO methods-based back analysis for elastic modulus of dam. Adv Eng Softw 2019;131:205–16. https://doi.org/10.1016/j.advengsoft.2019.02.005.
[25] Venkata Rao R. Jaya: A simple and new optimization algorithm for solving constrained and unconstrained optimization problems. Int J Ind Eng Comput 2016:19–34. https://doi.org/10.5267/j.ijiec.2015.8.004.
[26] Kang F, Liu X, Li J, Li H. Multi-parameter inverse analysis of concrete dams using kernel extreme learning machines-based response surface model. Eng Struct 2022;256. https://doi.org/10.1016/j.engstruct.2022.113999.
[27] Kang F, Wu Y, Li J, Li H. Dynamic parameter inverse analysis of concrete dams based on Jaya algorithm with Gaussian processes surrogate model. Adv Eng Inform 2021;49:101348. https://doi.org/10.1016/j.aei.2021.101348.
[28] Wang S, Xu Y, Gu C, Xia Q, Hu K. Two spatial association–considered mathematical models for diagnosing the long-term balanced relationship and short-term fluctuation of the deformation behaviour of high concrete arch dams. Struct Health Monit n.d.:19.
[29] Labibzadeh M, Khajehdezfuly A, Khayat M, Arab Y. Elastic Strength Diagnosis of the Dez Concrete Arch Dam Using Thermal Inverse Analysis. J Perform Constr Facil 2015;29:04014167. https://doi.org/10.1061/(ASCE)CF.1943-5509.0000660.
[30] Bao T, Li J, Lu Y, Gu C. IDE-MLSSVR-Based Back Analysis Method for Multiple Mechanical Parameters of Concrete Dams. J Struct Eng 2020;146:04020155. https://doi.org/10.1061/(ASCE)ST.1943-541X.0002602.
[31] Wang S, Xu C, Liu Y, Xu B. Zonal intelligent inversion of viscoelastic parameters of high arch dams using an HEST statistical model. J Civ Struct Health Monit 2022;12:207–23. https://doi.org/10.1007/s13349-021-00538-0.
[32] Dorafshan S, Azari H. Evaluation of bridge decks with overlays using impact echo, a deep learning approach. Autom Constr 2020;113:103133.

https://doi.org/10.1016/j.autcon.2020.103133.
[33] Oh BK, Glisic B, Kim Y, Park HS. Convolutional neural network - based wind - induced response estimation model for tall buildings. Comput-Aided Civ Infrastruct Eng 2019;34:843–58. https://doi.org/10.1111/mice.12476.
[34] Cha Y-J, Choi W, Büyüköztürk O. Deep Learning-Based Crack Damage Detection Using Convolutional Neural Networks: Deep learning-based crack damage detection using CNNs. Comput-Aided Civ Infrastruct Eng 2017;32:361–78. https://doi.org/10.1111/mice.12263.
[35] Zhang Y, Miyamori Y, Mikami S, Saito T. Vibration - based structural state identification by a 1 - dimensional convolutional neural network. Comput-Aided Civ Infrastruct Eng 2019;34:822–39. https://doi.org/10.1111/mice.12447.
[36] Léger P, Leclerc M. Hydrostatic, Temperature, Time-Displacement Model for Concrete Dams. J Eng Mech 2007;133:267–77. https://doi.org/10.1061/(ASCE)0733-9399(2007)133:3(267).
[37] Mata J. Interpretation of concrete dam behaviour with artificial neural network and multiple linear regression models. Eng Struct 2011;33:903–10. https://doi.org/10.1016/j.engstruct.2010.12.011.
[38] Salazar F, Morán R, Toledo MÁ, Oñate E. Data-Based Models for the Prediction of Dam Behaviour: A Review and Some Methodological Considerations. Arch Comput Methods Eng 2017;24:1–21. https://doi.org/10.1007/s11831-015-9157-9.
[39] Prakash G, Sadhu A, Narasimhan S, Brehe J-M. Initial service life data towards structural health monitoring of a concrete arch dam: Structural health monitoring of a concrete arch dam. Struct Control Health Monit 2018;25:e2036. https://doi.org/10.1002/stc.2036.
[40] Kang F, Liu J, Li J, Li S. Concrete dam deformation prediction model for health monitoring based on extreme learning machine. Struct Control Health Monit 2017;24:e1997. https://doi.org/10.1002/stc.1997.
[41] Ren Q, Li M, Kong T, Ma J. Multi-sensor real-time monitoring of dam behavior using self-adaptive online sequential learning. Autom Constr 2022;140:104365. https://doi.org/10.1016/j.autcon.2022.104365.
[42] Tatin M, Briffaut M, Dufour F, Simon A, Fabre J-P. Thermal displacements of concrete dams: Accounting for water temperature in statistical models. Eng Struct 2015;91:26–39. https://doi.org/10.1016/j.engstruct.2015.01.047.
[43] Bergstra J, Bengio Y. Random Search for Hyper-Parameter Optimization n.d.:25.
[44] Mckay MD, Beckman RJ, Conover WJ. A Comparison of Three Methods for Selecting Values of Input Variables in the Analysis of Output From a Computer Code. Technometrics 2000;42:55–61. https://doi.org/10.1080/00401706.2000.10485979.
[45] Olsson A, Sandberg G, Dahlblom O. On Latin hypercube sampling for structural reliability analysis. Struct Saf 2003;25:47–68. https://doi.org/10.1016/S0167-4730(02)00039-5.
[46] Flah M, Ragab M, Lazhari M, Nehdi ML. Localization and classification of structural damage using deep learning single-channel signal-based measurement. Autom Constr 2022;139:104271. https://doi.org/10.1016/j.autcon.2022.104271.
[47] Tseranidis S, Brown NC, Mueller CT. Data-driven approximation algorithms for rapid performance evaluation and optimization of civil structures. Autom Constr 2016;72:279–93. https://doi.org/10.1016/j.autcon.2016.02.002.

Tables

Table 1. Hyperparameters for CNN surrogate model

Parameter	Set
Optimizer	ADAM
Maximum number of epochs	100
Size of the mini-batch	32
Sequence length	50
Initial learn rate	1e-3
Learn rate drop period	'Piecewise'
Learn rate drop factor	0.1

Table 2. Results of displacement analysis models for different monitoring points

Monitoring points	Training			Test		
	MAE (mm)	RMSE (mm)	R^2	MAE (mm)	RMSE (mm)	R^2
PL10-2	0.7135	0.9889	0.9949	0.8898	1.0602	0.9928
PL10-3	0.6287	0.8717	0.9941	0.7699	0.9099	0.9919
PL10-5	0.1886	0.2446	0.9867	0.2018	0.2343	0.9931
PL15-1	0.8542	1.1497	0.9972	1.1612	1.3054	0.9936
PL15-2	0.7722	1.0614	0.9968	1.0840	1.2247	0.9923
PL15-4	0.5974	0.7883	0.9958	0.7404	0.8675	0.9877
PL15-5	0.3287	0.4031	0.9961	0.2774	0.3501	0.9899
PL22-1	1.0561	1.4434	0.9939	1.0306	1.2588	0.9877
PL22-2	1.0155	1.4079	0.9917	0.9847	1.1762	0.9846
PL22-4	0.9164	1.1815	0.9832	0.9827	0.8285	0.9618

Note: MAE is the mean absolute error, RMSE is the root mean squared error, R^2 is the coefficient of determination.

Table 3. Performance of the Jaya-CNN for forward analysis

Dam block	Monitoring point	Measured (mm)	Calculated (mm)	Absolute error (mm)	Relative error (%)
Block 10	PL10-2	24.7634	24.6512	0.1121	0.4529
	PL10-3	20.8242	21.2289	0.4047	1.9432
	PL10-5	31.5294	31.4631	0.0663	0.2104
Block 15	PL15-1	28.8865	28.7880	0.0985	0.3410
	PL15-2	18.5472	18.0832	0.4006	2.1598
	PL15-4	26.4008	26.1290	0.2718	1.0295
	PL15-5	22.9936	23.0047	0.0111	0.0487
Block 22	PL22-1	3.91424	3.9025	0.0117	0.2990
	PL22-2	8.6766	8.6627	0.0139	0.1596
	PL22-4	12.0977	12.0716	0.0262	0.2164

Table 4. Comparison of computational time with direct FE method

Items	Execution time (min)		Efficiency improvement (%)
	Direct FE	Proposed	
Sample set preparation	-	1072.75	-
Objective function Minimization	25746	1.03	-
Total	25746	1073.78	95.83

Table 5. Comparison of different surrogate models

Prediction error (mm)	CNN	BP	RBF	Performance improvement (%)	
				CNN vs BP	CNN vs RBF
Training MAE	0.0114	0.0486	0.1125	76.54	89.87
Training RMSE	0.0156	0.0660	0.1598	76.36	90.24
Test MAE	0.0175	0.0774	0.1261	77.39	86.12
Test RMSE	0.0244	0.1110	0.1821	78.02	86.60

Table 6. Result of parameter inverse analysis for different methods (GPa)

Method	E_A	E_B	E_C	E_{r1}	E_{r2}	E_{r3}
Jaya-CNN	53.799	45.733	37.374	39.657	24.816	42.359
PSO-CNN	51.749	47.393	39.047	40.883	25.419	42.322
GA-CNN	51.791	46.541	38.340	41.960	25.627	40.337
Jaya-BP	54.137	43.268	35.867	43.791	24.643	40.068
Jaya-RBF	53.620	43.679	36.090	42.673	24.925	40.047

Table 7. Performance comparison of different methods

Methods	Average absolute error (mm)	Average relative error (%)
Jaya-CNN	0.1417	0.6860
PSO-CNN	0.2379	1.1465
GA-CNN	0.1708	0.8899
Jaya-BP	0.2619	1.4609
Jaya-RBF	0.2549	1.3364

Figures

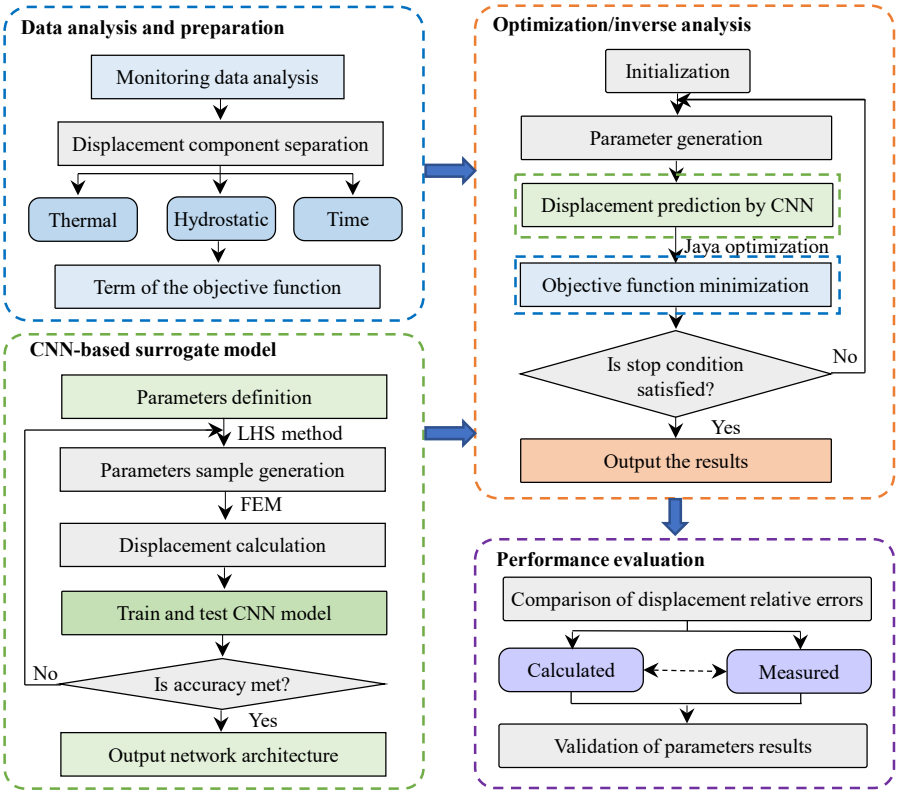

Fig. 1. Proposed framework for multi-zone parameter inverse analysis of super high arch dams

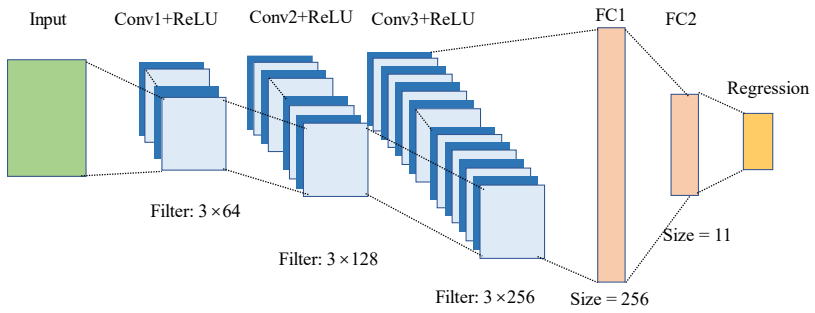

Fig. 2. Proposed architecture of CNN

Set the common controlling parameters of algorithm, including maximum number of iterations N_k, number of solutions N_S, number of optimization variables N_D, Search space domain $[B_l\ B_u]$.
Initialize solution $p_{i,j}$, i=1, 2, …, N_D, j= 1,2, …, N_S.
Calculate the fitness value of each solution $f(p_{i,j})$.
Number of iterations k =1.
While (k< K)
    Record the position of the best and worst solution
    For j=1: N
    Update solution to new one $p_{i,j}$ by Eq. (12)
    Tuning solutions within $[B_l\ B_u]$
        If ($f(p_{i,j}) < f(p_{i,j})$)
        $p_{i,j} = p_{i,j}^{new}$
        $f(p_{i,j}) = (p_{i,j}^{new})$
        Else
        Keep previous results
        End if
    End
    k=k+1
End while
Output optimization results

Fig. 3. Pseudocode of Jaya for optimization

Fig. 4. The concrete arch dam

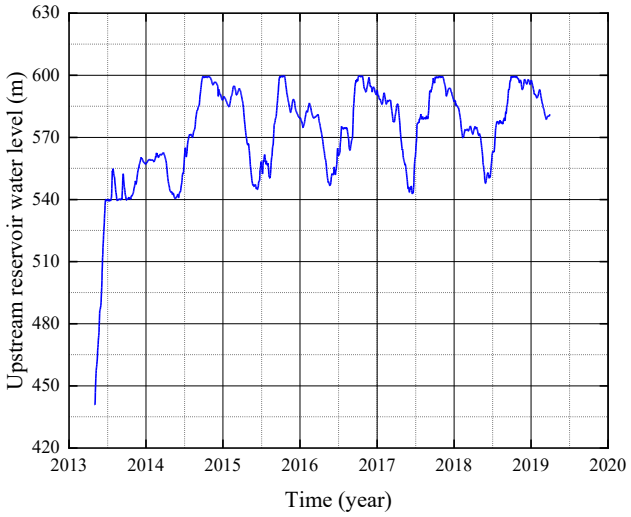

Fig. 5. Variation curve of upstream reservoir water level

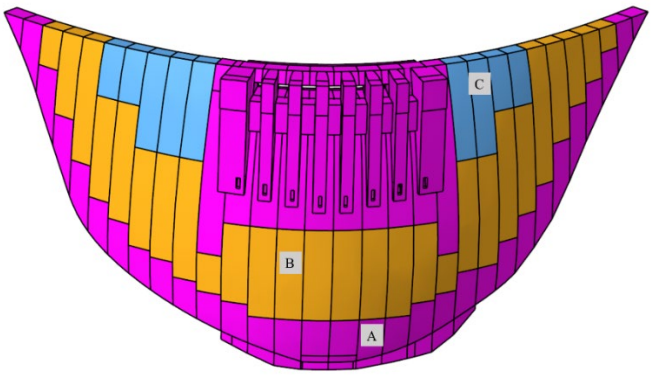

Fig. 6. Zoning of the dam for finite element modeling

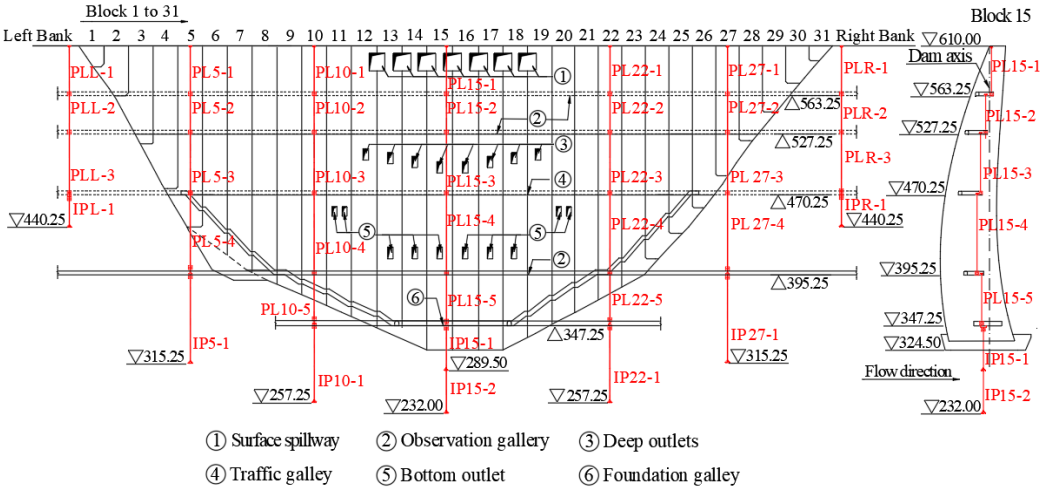

Fig. 7. Pendulum system for dam horizontal displacement monitoring. PL is the plumb line, and IP is the Inverted plumb line.

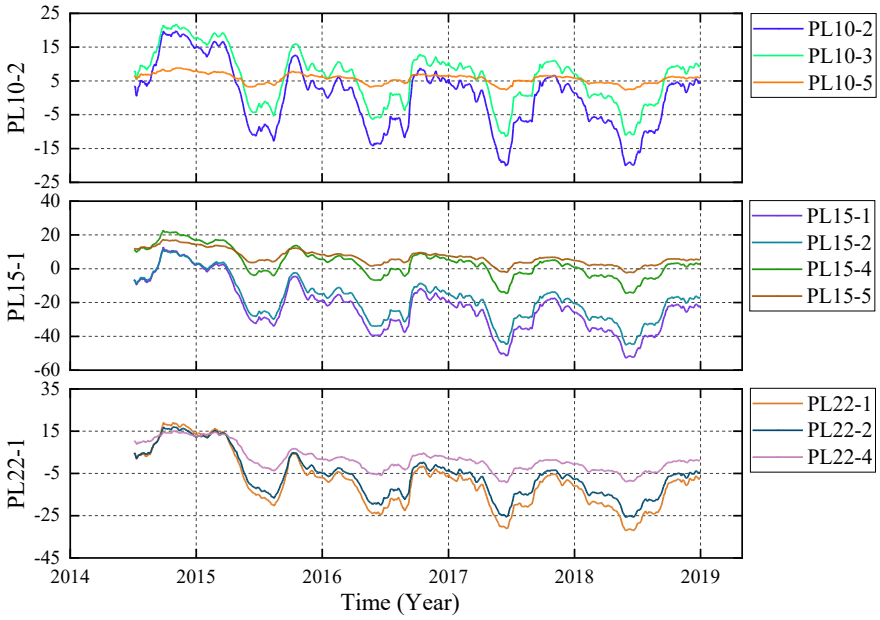

Fig. 8. Horizontal radial displacements (downstream is positive) at the selected monitored points

625

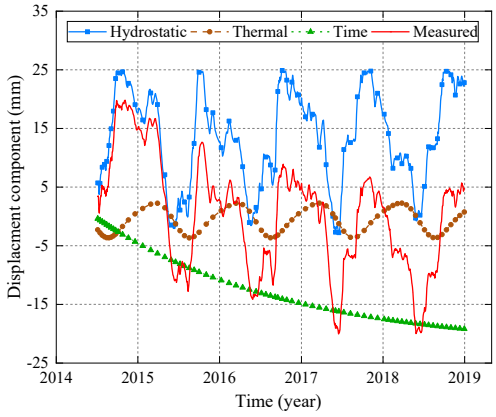

(a)

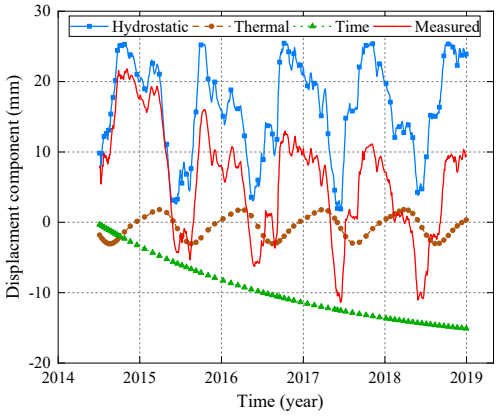

(b)

626

627

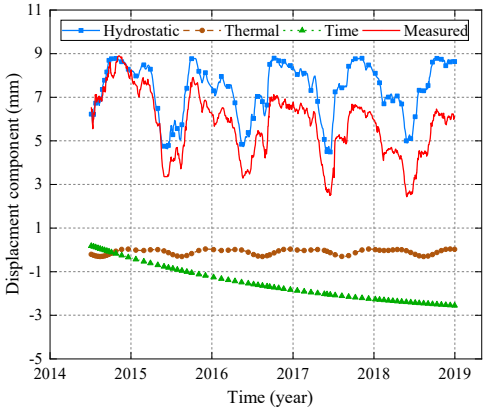

(c)

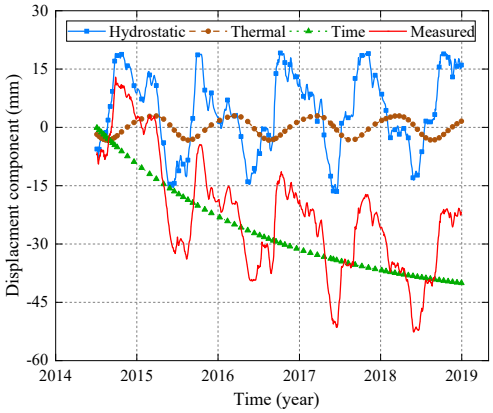

(d)

628

629

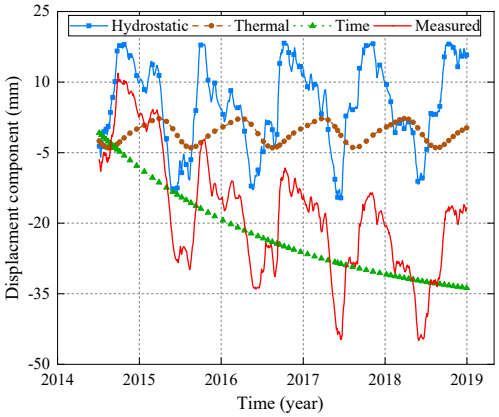

(e)

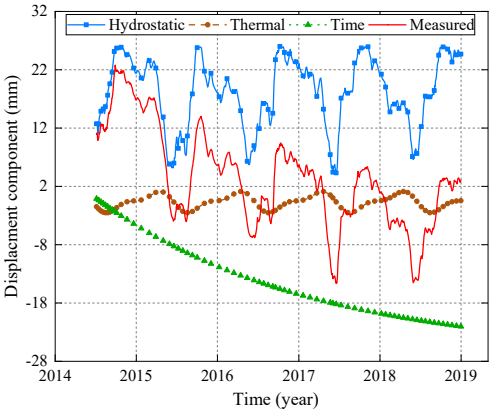

(f)

630

631

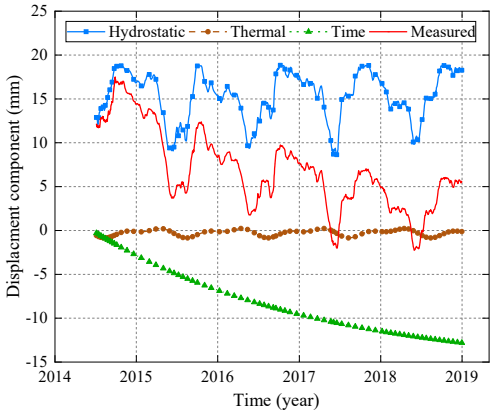

(g)

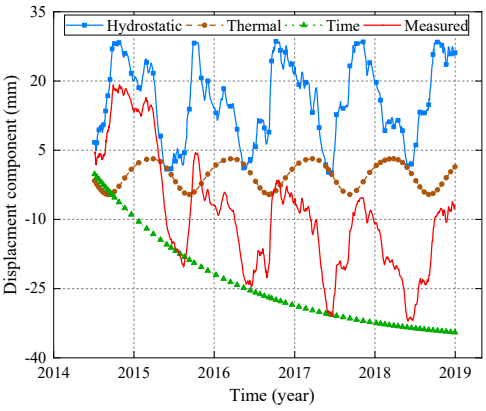

(h)

632

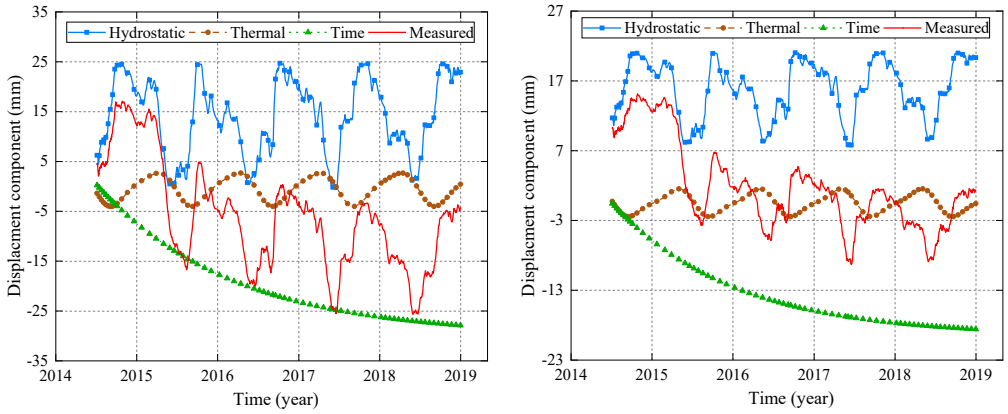

Fig. 9. Component separation of displacement. (a) PL10-2; (b) PL10-3; (c) PL10-5; (d) PL15-1; (e) PL15-2; (f) PL15-4; (g) PL15-5; (h) PL22-1; (i) PL22-2; (j) PL22-4

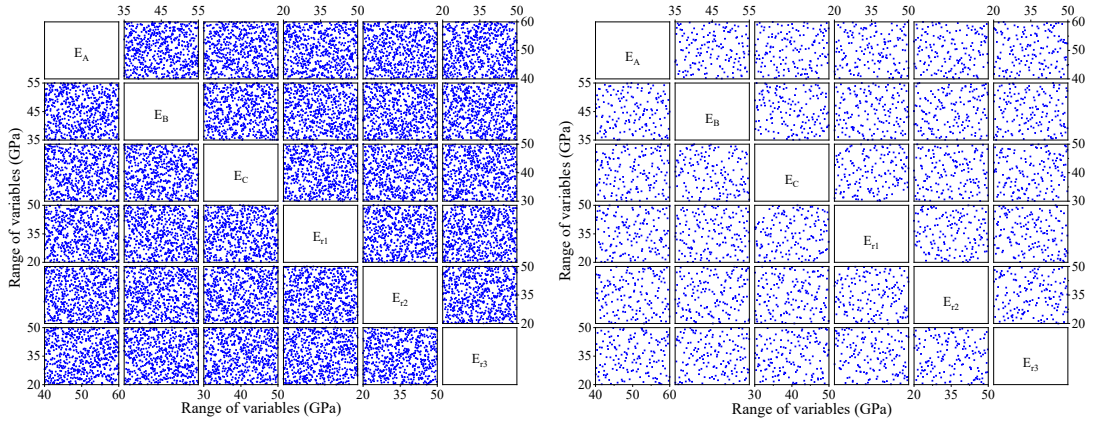

Fig. 10. Pairwise distribution of sample sets by LHS. (a) Training sampling; (b) Test sampling

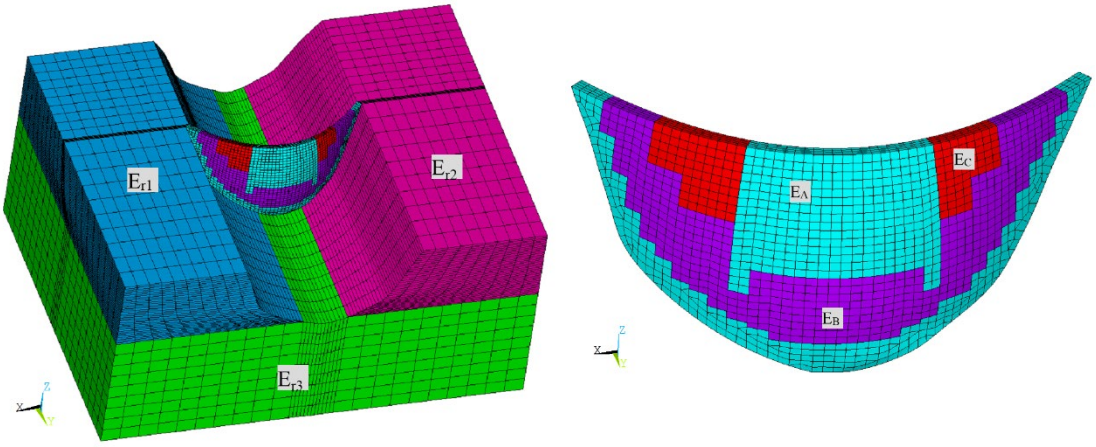

Fig. 11. Parameter setting and FEM of dam-foundation system. (a) Dam and foundation; (b) Dam body

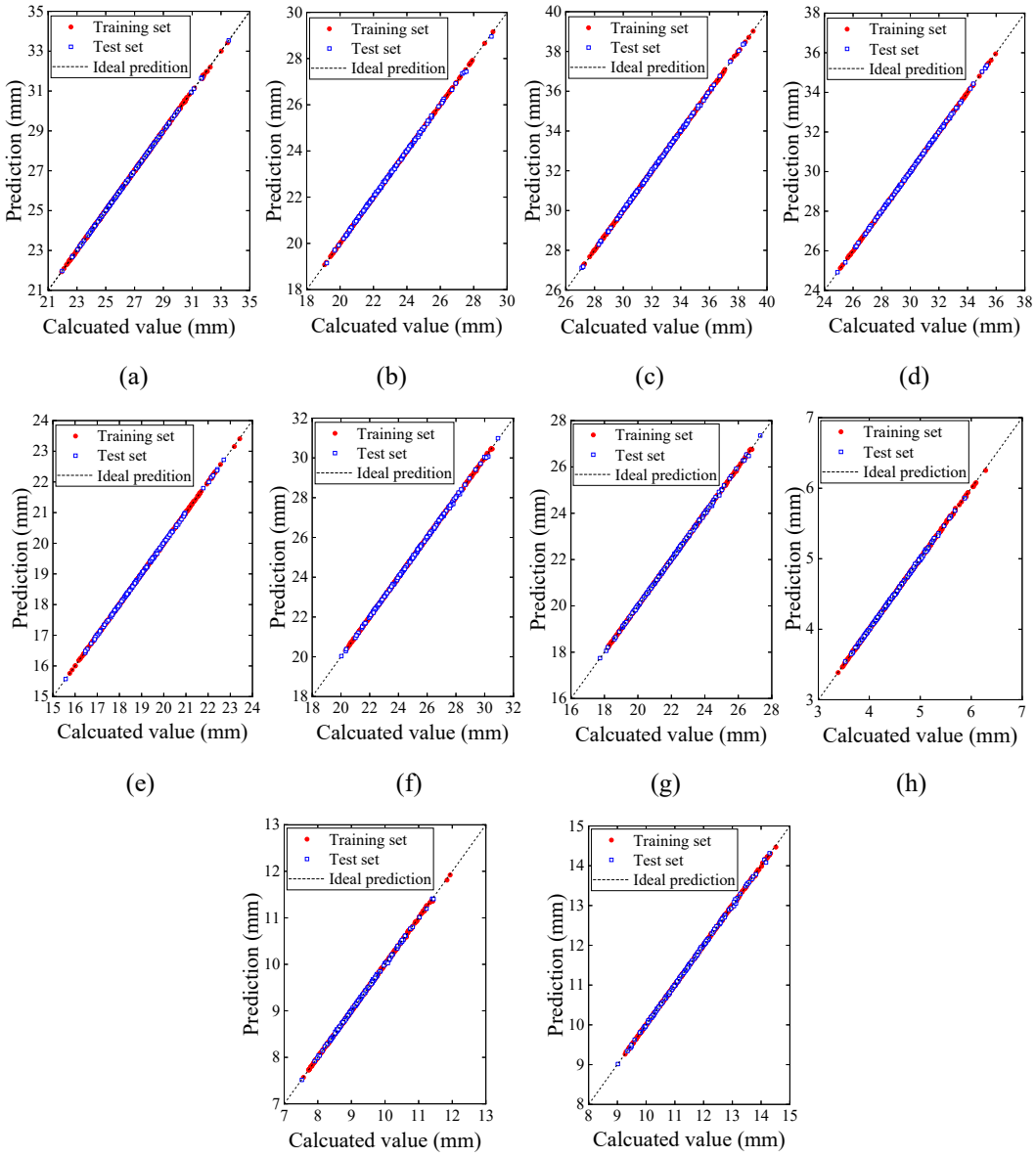

Fig. 12. Results predicted by the CNN-based surrogate model versus calculated by the FEM. (a) PL10-2; (b) PL10-3; (c) PL10-5; (d) PL15-1; (e) PL15-2; (f) PL15-4; (g) PL15-5; (h) PL22-1; (i) PL22-2; (j) PL22-4

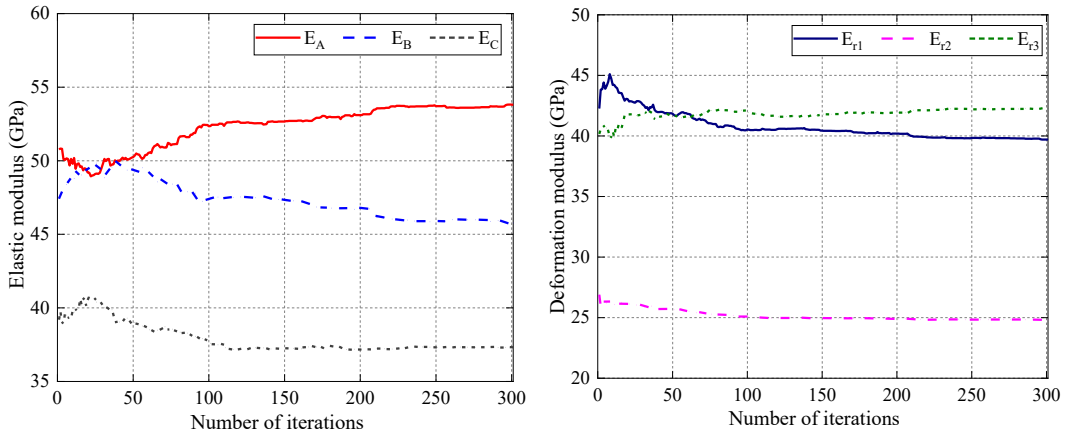

(a) (b)

Fig. 13. Process of parametric inverse analysis of the proposed method. (a) Elastic modulus of dam; (b) Deformation modulus of foundation

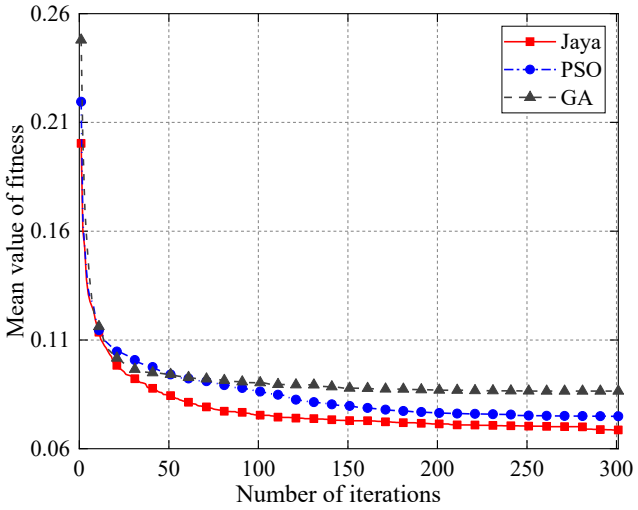

Fig. 14. Comparison of the best mean fitness evaluation process for different algorithms

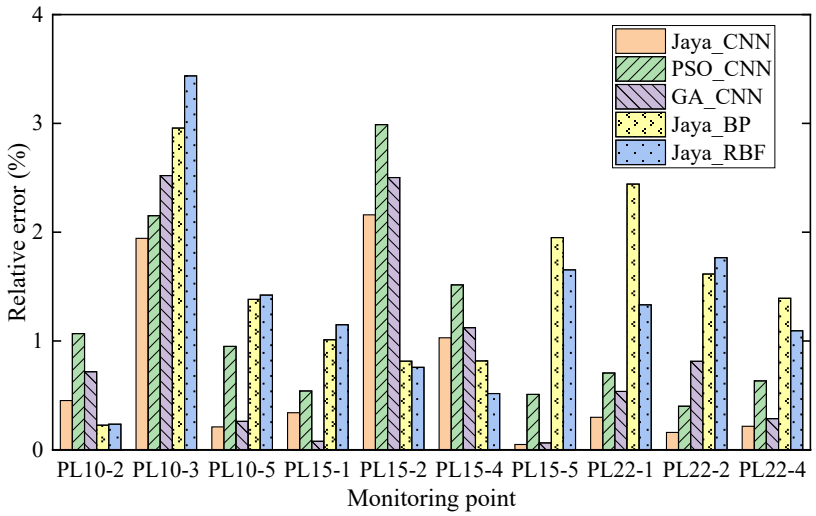

Fig. 15. Comparison of different methods based on absolute errors of hydrostatic component